Alcohol Promotes Hepatocellular Carcinoma Metastasis Through SIRT7-Dependent EMT Regulation

Chen Zhang
Hunan Normal University School of Medicine
Jinqiu Zhao
The First Affiliated Hospital of Chongqing Medical University
Jie Zhao
: University of Kansas Medical Center Department of Internal Medicine
Bohao Liu
Hunan Normal University School of Medicine
Wenbin Tang
Hunan Normal University School of Medicine
Yi Liu
People's Hosipital of Hunan Province
Wenxiang Huang
First Affiliated Hospitak of Chongqing Medical University
Steven A Weinman
Department of Internal Medicine,and Liver Center,University of Kansas Medical Center
ZHUAN LI (zhuanli@hunnu.edu.cn)
Hunan Normal University School of Medicine https://orcid.org/0000-0002-1310-4584

Research

Keywords: epigenetic, Sirtuin protein, HDAC III deacetylase, therapeutic target

Posted Date: November 10th, 2021

DOI: https://doi.org/10.21203/rs.3.rs-983099/v1

Abstract

Background

Long-term alcohol use is a confirmed risk factor of liver cancer tumorigenesis and metastasis. Multiple mechanisms responsible for alcohol related tumorigenesis have been proposed, including toxic reactive metabolite production, oxidative stress and fat accumulation which trigger hepatocyte cell death and inflammation. However, mechanisms underlying alcohol-mediated liver cancer metastasis remain largely unknown.

Methods

SIRT7 expression pattern and its association with HCC metastasis were investigated by bioinformatic analysis and verified by western blot and immunochemistry in HCC tissues. The biological consequences of overexpression and knockdown of SIRT7 in HCC metastasis were studied *in vitro* and *in vivo*. qRT-PCR, immunofluorescence assay, ChIP assay were utilized to assess the effects of SIRT7 on E-cadherin expression. Effects of alcohol on SIRT7 expression were evaluated by qRT-PCR, immunofluorescence and inhibitor treatments and pulmonary metastasis model mice fed with Lieber Decarli alcohol diet were used to clarify the mechanisms by which SIRT7 facilitated alcohol mediated HCC metastasis.

Results

SIRT7 is a critical factor in promoting liver cancer metastasis. SIRT7 expression is closely associated with disease stage and high SIRT7 predicts worse overall and disease-free survival. Overexpression of SIRT7 promotes HCC cell migration and EMT while knockdown of SIRT7 showed opposite effects. Mechanistically, we found that SIRT7 suppresses E-Cadherin expression through promoter binding and H3K18 deacetylation. Most importantly, we identified that alcohol upregulates SIRT7 expression in hepatocyte both *in vitro* and *in vivo*. Reducing SIRT7 activity completely abolished alcohol-mediated liver cancer metastasis *in vivo.*

Conclusion

SIRT7-dependent EMT regulation is a pivotal regulatory mechanism of alcohol-mediated HCC metastasis and reveals previously unidentified roles of SIRT7 in promoting EMT and metastasis in human HCC. Therapeutic strategies that inhibit SIRT7 may offer novel options for the treatment of HCC.

Background

Hepatocellular carcinoma (HCC), the most common pathological form of primary liver cancer, accounts for the fifth leading cause of cancer-related human death worldwide and its incidence still increasing (1).

Despite great efforts that have been made during the last decades to improve diagnosis and treatment for intrahepatic lesions, advanced HCC often has a poor prognosis with a five-year survival rate less than 18% mainly due to drug resistance, tumor metastasis and recurrence (1, 2). While extensive research has identified a number of molecular biomarkers, cellular networks and signaling pathways affected in liver cancer, mechanisms underlying tumor metastasis are poorly understood (2).

Alcohol is a confirmed risk factor of liver cancer and long-term alcohol use has been linked to an increased risk of liver cancer tumorigenesis as well as distant metastasis(3–6). Multiple mechanisms are responsible for alcohol related tumorigenesis, including production of toxic reactive metabolites, oxidative stress and fat accumulation in hepatocytes. All of those pathological changes result in hepatocyte death, inflammation, fibrosis deposition and ultimately liver cancer (4, 7, 8). Emerging evidence has suggested that long term alcohol use causes cancer stem cell activation and epithelial-mesenchymal transition (EMT) which facilitates liver cancer cell metastasis (6, 9). However, factors and mechanisms underlying alcohol-mediated liver cancer metastasis remaining largely unknown.

Epithelial mesenchymal transition (EMT) is the most common feature when advanced cancer initiates metastasis (10, 11). In the case of HCC, EMT is utilized by liver cancer cells to initiate metastatic spread. After EMT, liver epithelial cells lose cell-to-cell adhesion and become motile mesenchymal cells, which allows for the migration from the primary tumor site to establish distant metastasis (12). A critical molecular feature responsible for liver cancer cell EMT is the downregulation of E-cadherin. E-cadherin is a cell adhesion molecule present in most normal epithelial cell plasma membranes but it is frequently repressed or degraded in various type of human cancer cells (13). Mechanisms underlying the functional loss of E-cadherin in cancer cells include posttranslational loss of protein function, transcriptional silencing due to promoter hypermethylation, and the activation of several transcription repressors of E-cadherin, such as Snail, Slug, Sip1 and Ets (13, 14). Previous studies have shown that alcohol was able to promote liver cancer EMT and metastasis but the factors and mechanisms underlying alcohol mediated EMT remain largely unknown (6, 9).

SIRT7 is a family member of the silent information regulator (Sir2) proteins that are described as NAD^+-dependent class III histone deacetylases (HDAC3). Compared with other family members like SIRT1 and SIRT6, the enzymatic activity and functions of SIRT7 are poorly understood. SIRT7 is the only Sir2 family member that is predominantly localized in the nucleus where it regulates RNA polymerase I transcription by acting as an H3K18 deacetylase (15). Besides H3K18, SIRT7 has also been reported to target several non-histone proteins, including p53 (16), GABP-β (17), FOXO3 (18) and U3-55k (19) for deacetylation, and has been implicated in multiple cellular functions including hepatic lipid metabolism, mitochondrial homeostasis and adipogenesis. Emerging evidence has also implicated SIRT7 in various aspects of cancer biology (20–22). H3K18 deacetylation by SIRT7 is important for maintaining the fundamental properties of the cancer cell phenotype (20). Knockdown of SIRT7 influences cell cycle control and causes an increased proportion of cancer cells that remain in the G1/S phase (15, 20, 21). In epithelial prostate carcinomas, high SIRT7 levels are associated with metastatic disease and poor prognosis (22).

In HCC, SIRT7 expression is also upregulated in a large cohort of HCC patents (21) and we have identified elevated SIRT7 expression is associated with chemosensitivity by regulating TP53 activity(23).

In the present study, we further demonstrated that SIRT7 as a critical regulator of liver cancer metastasis. Our findings revealed that high SIRT7 levels are associated with metastasis in human HCC. SIRT7 regulates HCC EMT and suppresses E-Cadherin transcription. Our data also suggested that alcohol upregulates SIRT7 expression in both human primary hepatocytes and alcohol-fed mice liver in CYP2E1-dependent mechanism. Reducing SIRT7 activity significantly prevented alcohol-mediated liver cancer metastasis *in vivo.* The current findings present a novel mechanism that controls alcohol-mediated HCC metastasis and reveals SIRT7 as a pivotal regulatory factor in regulating EMT and determining metastasis in human HCC. Therapeutic strategies that inhibit SIRT7 may offer novel options for the treatment of HCC.

Materials And Methods

Cell culture, plasmids and transfection

Huh7.5 cells were provided by Dr. Charles Rice, (Rockefeller University, New York, NY, USA), HepG2 cells were provided by Dr. Tiangang Li (University of Kansas Medical Center, Kansas, KS), SK-Hep1 cells were purchased from ATCC (Manassas, VA). All cells were maintained in Dulbecco's modified Eagle's medium (Invitrogen, Grand Island, NY) containing 10% fetal bovine serum (FBS), 50 U/ml penicillin and 50 mg/ml streptomycin. Flag-SIRT7, proE-cad670-Luc (E-cadherin promoter region from -670 to +92) plasmids were respectively provided by Drs Eric Verdin, Kumiko Ui-Tei via Addgene (Cambridge, MA). To generate mutants of E-cadherin luciferase reporter plasmids, proE-cad670-Luc was used as template and mutants were reconstituted by using the Q5 Site-Directed Mutagenesis Kit from New England BioLabs (Ipswich, MA). Cells were transfected in serum-free medium (Opti-MEM, Invitrogen) by using X-tremeGENE™ HP DNA Transfection Reagent (Roche, Indianapolis, IN) as previously described(24). siRNA targeting SIRT7 (SMARTpool: ON-TARGET plus human SIRT7 siRNA), shRNA targeting SIRT7 (MISSION® esiRNA targeting human SIRT7) and shRNA targeting FOXO3 (MISSION® TRC shRNA TRCN0000040100) were purchased from GE Dharmacon (Lafayette, CO) and Sigma-Aldrich (St. Louis, MO), respectively.

Antibodies and Chemicals

Anti-SIRT7 (D3K5A), anti-SIRT1 (D1D7), anti-β-actin (8H10D10), anti-FOXO3 (75D8), anti-E-cadherin (24E10) were purchased from Cell Signaling Technology (Boston, MA). Anti-GAPDH (FL-335) anti-α-SMA (SC53124) and anti-Vimentin (SC6260) were purchased from Santa Cruz Biotechnology (Dallas, TX). Anti-beta actin (AC-15), and anti-Flag (M2) were purchased from Sigma-Aldrich. Anti-SIRT7 (PA5-87543) was purchased from Invitergen. Daidzin, Fomepizole, dially sulfide (DAS), N-acetyl-L-cysteine (NAC), 4-Hydroxynonenal (4-HNE) were purchased from Sigma-Aldrich.

Animal model

Male NSG mice (4 weeks of age) were purchased form The Jackson Laboratory (Bar Harbor, ME) and Gempharmatech (Nanjing, China). Mice were housed in a temperature-controlled, pathogen-free environment with 12-hour light-dark cycles. All animal handing procedures were approved by the Institutional Animal Care and Use Committees at The University of Kansas Medical Center (Kansas City, KS) and Hunan Normal University School of Medicine (Changsha, China).

Mice received a single tail vein injection of $1x10^6$ cells suspended in 100 µL DMEM and tumor formation was determined in lung 4 weeks after injection by using Hematoxylin &Eosin (H&E) staining. Alcohol feeding procedures were previously described (25). One week after cell injection, mice were initially fed the control Lieber-DeCarli diet ad libitum for 5 days to acclimatize them to a liquid diet. Then mice were subsequently allowed free access to the ethanol Lieber-DeCarli Diet containing 5% (vol/vol) ethanol for 2 weeks, and control-fed groups were pair-fed with an isocaloric control diet. All mice were sacrificed 4 weeks after injection and lungs were collected for determining tumor formation. Liver sections from CYP2E1$^{-/-}$ and control mice were kindly provided by Dr. Laura Nagy as previously described (26).

Human specimens and immunohistochemistry

De-identified human liver specimens from liver explants were obtained from The University of Kansas Medical Center, The First Affiliated Hospital of Chongqing Medical University, and The Affiliated Hospital of Hunan Normal University (People's Hospital of Hunan Province). Written informed consent was obtained from all patients and all studies using human tissue samples were approved by the Human Subjects Committee of the University of Kansas Medical Center, Chongqing Medical University and Hunan Normal University School of Medicine.

Immunohistochemistry was performed as previously described(23, 25). After deparaffinization and rehydration, antigen retrieval was achieved by heating in a pressure cooker for 5 min in 10mM of sodium citrate (pH6). Peroxidase activity was blocked by incubation in 3% H2O2 for 10 minutes. Sections were rinsed three time in PBS/PBS-T (0.1% Tween-20) and incubated in Dako Protein Block (Dako, Agilent Technologies, Santa Clara, CA) for 10 minutes. After removal of blocking solution, slides were placed into a humidified chamber and incubated overnight with primary antibodies in blocking buffer (4% normal goat serum in PBS) and incubated over night at 4 °C. After washing, slides were covered with SignalStain Boost IHC Detection Reagent (Cell Signaling Technologies, Boston, MA) for 30 min at room temperature. After washing two times with PBS-T, the Substrate-Chromgen Solution (VECTOR NovaRED, Substrate Kit, Vector Laboratories, Burlingame, CA) was applied, slides were incubated 5-10 min and counterstained with Hemtoxylin. Images were acquired using a Nikon Eclipse 80i microscope (Nikon Americas Inc., Melville, NY).

Isolation of human and mouse primary hepatocyte

Primary human hepatocytes were freshly isolated from liver resections as previously described (24, 27) by the Cell Isolation Core of the Department of Pharmacology at the University of Kansas Medical Center. All human tissues were obtained with informed consent from each patient, according to ethical

and institutional guidelines. The study was approved by the Institutional Review Board at the University of Kansas Medical Center.

Mouse primary hepatocyte were isolated by using a multi-step collagenase procedure (27). In brief, the liver was perfused with calcium-free solution and then digested with a collagenase (Sigma-Aldrich) perfusion. Dispersed cells were released from the isolated liver, hepatocytes were collected by 50×g centrifugation and then seeded on collagen coated plates and allowed to attach in a humidified 37 °C, 5% CO_2 incubator for 12 h and treated with 50mM ethanol for indicated times

Quantitative polymerase chain reaction (qRCR)

Total RNA was isolated from cells using the TRIzol reagent (Thermo Fisher Scientific, Inc.), followed by cDNA synthesis using an RNA reverse transcription kit (Applied Biosystems; Thermo Fisher Scientific, Inc.). Subsequently, a CFX96 real-time system (Bio-Rad, Hercules, CA, USA) was used to perform qPCR. Reaction volumes of 20 µl were used, containing 10µl of the SYBR Green PCR master mix (Applied Biosystems; Thermo Fisher Scientific, Inc.). Primer sequences for human SIRT7 and E-cadherin are as following: SIRT7-forward: *5′-GACCTGGTAACGGAGCTGC-3′,* SIRT7-reverse:*5′-CGACCAAGTATTTGGCGTTCC-3′;* E-cadherin forward: *5′- GGGGTCTGTCATGGAAGGTG -3′*, E-cadherin reverse: *5′- CAAAATCCAAGCCCGTGGTG -3′;*GAPDH forward:*5′-GAAGGTGAAGGTCGGAGTC-3′,* GAPDH reverse: *5′-GAAGATGGTGATGGGATTTC-3′.*

Chromatin immunoprecipitation (ChIP) assay

ChIP assays were performed as described previously(23, 24). Briefly, cells were fixed, washed, and harvested, followed by shearing of genomic DNA by sonication. Sonicated DNA (20 µl) was purified and 1% of DNA was used as input DNA control. Chromatin-bound DNAs were immunoprecipitated using antibodies as indicated. The eluted DNA from the beads was precipitated and analyzed by PCR using multiple primer sets as following: pro-Ecad A forward: *5′-GGCTGCTAGCTCAGTGGCTC-3′,* pro-Ecad A reverse: *5′-TGGGCTCAAGCGGTCCTCT-3′;* pro-Ecad B forward: *5′-AACTCCAGGCTAGAGGGTCACC-3′,* pro-Ecad B reverse: *5′- GGCTGGAGTCTGAACTGACTTCC -3′*

Western blot analysis

Total cell lysates prepared from cells were used for detection. Briefly, cells were washed twice with chilled PBS and then cell lysis was performed using the RIPA buffer (50 mM Tris, pH 7.5, 150 mM sodium chloride, 1% NP-40, 0.2% SDS, 0.5% sodium deoxycholate, 0.1 mM EDTA, and 1% protease and phosphatase inhibitors (Sigma-Aldrich). After centrifugation at 16,000 *g* for 15 min, supernatants were collected. Cell lysates (25 µg) were separated on a 10% SDS-PAGE and transferred to polyvinylidene difluoride membranes (Immobilon-P membranes; EMD Millipore, Billerica, MA, USA). Membranes were blocked with blocking buffer (5% skim milk, 0.1% Tween-20 in PBS) for 1 h at room temperature. Following incubation with primary antibodies (1:1000) overnight at 4°C, the membranes were incubated with horseradish peroxidase-conjugated secondary antibodies (Thermo Fisher Scientific, Inc. Waltham,

MA, USA). Signals were detected using the ECL Western Blotting Detection system (Thermo Fisher Scientific, Inc).

Immunofluorescence

For indirect immunofluorescence, cells grown on coverslips were fixed with 4% paraformaldehyde at room temperature for 5 min and 0.2% Triton X-100 was used for cell permeation. The coverslips were inverted on 40-μl droplets of the blocking buffer (4% goat serum) and incubated at room temperature for 45 min to prevent non-specific binding. Subsequently, cells were incubated with primary antibodies for 1 h at room temperature. Coverslips were washed with PBS, followed by incubation for 1 h at room temperature in the dark with Alexa Fluor-conjugated secondary antibodies (1:5,000; Molecular Probes; Thermo Fisher Scientific, Inc.). Additionally, Dihydrochloride (DAPI) was added for 5 min at room temperature to stain nuclear DNA. Images were acquired using a Nikon Eclipse microscope (Nikon Corporation, Tokyo, Japan).

Wound healing assay

2×10^4 cells were plated in 24-well plates. When cells reached 100% confluence, sterile pipette tips (100 μl) were used to scratch the wound. Cell motility was assessed by measuring the movement of cells into the scratched wound after 24h incubation.

Migration assay

The 24-well transwell plates (0.4 μm pore size, Corning, Tewsbury, MA) were used to measure the migration ability of the cells. HCC cells (2×10^3) in 200 μl FBS-free media were added into the upper chamber, whereas 600 μl of the media with 10% FBS was added into the bottom chambers. Cells were fixed with methanol after a 48h incubation. Cells left on the membrane in the top chamber side were wiped off with a cotton swab, whereas the cells that migrated through the membrane were stained with crystal violet. The number of migratory cells in 10 random fields was counted under a microscope.

Statistical Analysis

Data are presented as mean ± sem. Statistical significance between groups was calculated by using one-way ANOVA followed by Turkey's test. Statistical significance between two groups was calculated by 2-tailed unpaired Student's t-test. Variance between groups met the assumptions of the appropriate test. Unless otherwise stated, a P-value of <0.05 was considered statistically significant. The Kaplan–Meier method was used to estimate the survival rates for SIRT7 expression. Equivalences of the survival curves were tested by log-rank statistics.

Results

Aberrantly increased SIRT7 expression was associated with HCC metastasis and poorer survival. To confirm clinical significance of SIRT7 in HCC patients, We first analyzed RNA sequencing data collected from The Cancer Genome Altas (TCGA) public database. The results showed that SIRT7 expression was

increased in HCC tissues and positively correlated with disease progression except stage IV due to limited sample size (Fig. 1A). The Kaplan–Meier method (using the log-rank test) also suggested that lower SIRT7 expression was associated with increased overall survival (Fig. 1B) and disease-free survival (Fig. 1C) compared with those of patients with higher levels of SIRT7. To further evaluate whether SIRT7 contributed to HCC metastasis, we collected HCC tumor samples from patients who underwent surgical resection or transplantation and examined SIRT7 expression by IHC and western blot. Consistent with our previous observations, we found that SIRT7 expression in tumors showing evidence of vascular invasion was significantly higher than in tumors that lacked this more aggressive, metastasis-promoting feature (Fig. 1D). IHC staining results indicated that in both normal and cirrhotic liver sections, SIRT7 staining was undetectable. However, SIRT7 showed positive staining in HCC and strong nuclear staining in metastatic HCC tissue (Fig. 1E).

SIRT7 is critical for HCC metastasis both in vitro **and in** vivo. To further confirm the role of SIRT7 in HCC metastasis, we knocked down SIRT7 in HCC cells using siRNA (Fig. 2A) and evaluated cell migration by using a wound healing and migration assay. Knockdown of SIRT7 significantly impaired the cell migration capability in Huh7 and HepG2 cells compared with those of controls (Fig. 2B-D). We further stably knocked down SIRT7 in SK-Hep1 cells with two different lentiviruses (shSIRT7#1 and shS IRT7#2) and evaluated whether SIRT7 regulates HCC metastasis *in vivo* using a xenograft model of pulmonary metastasis (Fig. 2E-G). We found that knockdown of SIRT7 markedly decreased lung metastasis compared with controls (shTRC, Fig. 2F and G). In contrast, overexpression of SIRT7 in HepG2 cells resulted in a significant increase of lung metastasis compared with formed by control cells (UT, $p<0.001$, Fig. 2H and I).

SIRT7 promotes EMT in HCC. To explore whether SIRT7 promoted HCC cell migration and metastasis by regulating EMT of HCC, we examined EMT associated markers in HCC cell lines using western blotting analysis. As expected, significantly downregulated E-cadherin and upregulated vimentin were observed in Huh7 cells overexpressed SIRT7 compared with those transfected with empty vectors (EV). Knockdown SIRT7 showed the opposite effects (Fig. 3A). Immunofluorescence showed similar results of SIRT7 knockdown and demonstrated increased E-cadherin and pan-claudin and decreased vimentin levels (Fig. 3B). We further performed western blot and IHC staining to compare expression of SIRT7, E-cadherin and vimentin in HCC samples with or without metastasis (Fig. 3C-E). Higher SIRT7 levels were present in metastatic HCC samples compared with non-metastatic HCC tissue. SIRT7 expression patterns were negatively correlated with E-cadherin expression level (Fig. 3C and D). Spearman correlation analysis showed a strong negative correlation between SIRT7 and E-cadherin ($R=-0.566$, $p<0.05$). We also analyzed RNA sequencing data collected from the TCGA and the results also showed negative correlation between SIRT7 and E-cadherin ($R=-0.1287$, $p<0.008$) (Fig. 3F). Kaplan–Meier method suggested that lower E-cadherin expression was associated with decreased overall survival (Fig. 3G). Most importantly, high expression of SIRT7 and low E-cadherin was associated with the lowest survival probability (Fig. 3H).

SIRT7 induces H3K18 deacetylation and suppresses E-cadherin via a FOXO3-dependent mechanism. Downregulation of E-cadherin is pivotal process of EMT in cancer cells and our data indicated that SIRT7 overexpression reduced E-cadherin expression. We thus sought to determine the mechanisms of SIRT7 suppression of E-cadherin. Overexpression of SIRT7 significantly decreased transcriptional activity of the E-cadherin promoter (Fig. 4A), indicating that SIRT7 suppresses E-cadherin at a transcriptional level. To assess whether SIRT7 binds to the E-cadherin promoter we performed ChIP assays. As shown in Fig. 4B, SIRT7 showed positive binding to E-cadherin promoter compared with IgG and this binding was significantly abolished in cells treated with siSIRT7. SIRT7 is involved in deacetylating H3K18 and this is responsible for gene silencing and maintenance of oncogenic transformation in human cancer cells. W thus next examined whether SIRT7 suppresses E-cadherin through similar mechanisms and performed ChIP assays measuring H3K18 acetylation levels at the E-cadherin promoter region. The results show that knockdown of SIRT7 resulted in significantly elevated H3K18 but not H3K56 acetylation level (Fig. 4C). This demonstrates that SIRT7 is responsible for H3K18 deacetylation at the E-cadherin promoter.

We further sought to determine how SIRT7 is recruited to the E-cadherin promoter since SIRT7 lacks known sequence-specific DNA binding domains (20). We analyzed E-cadherin promoter regions and identified FOXO3, ELK4 binding sites and E-box within this region. We thus made a series of mutants and performed luciferase assays to investigate whether those sites are required for SIRT7-mediated E-cadherin repression (Fig. 4D). The results showed that overexpression of SIRT7 suppressed transcriptional activity of E-cadherin. Mutations of E-box or ELK4 showed no effect on SIRT7-dependent repression. However, mutants of either FOXO3 binding site completely abolished SIRT7-mediated suppression (Fig. 4E). To further address whether FOXO3 is required for SIRT7-mediated E-cadherin repression, we knocked down FOXO3 (Fig. 4E) and performed luciferase assays in those cells. As expected, in the absence of FOXO3, SIRT7 no longer suppressed transcriptional activity of E-cadherin compared with empty vectors (Fig. 4F). We further investigated expression of FOXO3 and SIRT7 patterns in determining disease progression in human liver cancer and Kaplan–Meier method suggested that high FOXO3 expression were associated with decreased overall survival (Fig. 4G) and disease-free survival (Fig. 4H) compared with those of patients with lower levels of FOXO3. Most importantly, high expressions of SIRT7 and FOXO3 was associated with the lowest survival probability while low expressions of SIRT7 and FOXO3 were associated with the highest survival probability compared with other expression patterns, respectively (Fig. 3H).

Elevated SIRT7 expression in hepatocytes upon ethanol exposure. Alcohol is well known to promote HCC metastasis (9, 28) and our results indicated that SIRT7 is also critical for HCC metastasis. We thus evaluated whether alcohol promotes HCC metastasis through SIRT7. To test this hypothesis, we first determined whether ethanol treatment modulates SIRT7 expression in HCC cells. Consistent with a previous report (29), ethanol treatment of HCC cells resulted in downregulation of SIRT1 expression, but SIRT7 expression was significantly upregulated in both SK-Hep1 and Hep3B cells (Fig. 5A). Elevated mRNA levels of SIRT7 were also observed in SK-Hep1 cells starting from 24h after alcohol exposure (Fig. 5B), indicating ethanol treatment regulates SIRT7 at a transcriptional level. In primary human and mouse hepatocytes, ethanol treatment resulted in increased SIRT7 expression and concomitantly

decreased E-cadherin expression (Fig. 5C). We further examined SIRT7 expression in alcohol fed mouse liver and the results showed that alcohol feeding increased SIRT7, and decreased E-cadherin expression compared with a control diet (Fig. 5D). To address whether alcohol feeding increased SIRT7 expression in hepatocytes, we isolated hepatocytes from mouse liver and analyzed protein levels by western blot, the results indicated that alcohol feeding increases SIRT7 expression but suppressed E-cadherin expression in hepatocytes (Fig. 5E).

Cyp2E1-dependent oxidative stress is responsible for alcohol mediated SIRT7 induction. To determine whether alcohol dehydrogenase and cytochrome P450-dependent oxidizing systems were responsible for SIRT7 induction, we first treated cells with acetaldehyde (ALD) or ethanol in the presence of inhibitors of either aldehyde dehydrogenase (ALDH) alcohol dehydrogenase (ADH) or Cyp2E1 and measured SIRT7 mRNA levels (Fig. 6A). We found that ethanol increased SIRT7 mRNA level almost 3-fold but ALD treatment did not change SIRT7 mRNA level. The Cyp2E1 inhibitor (Cyp2E1 inhi) alizarin completely abolished ethanol induced SIRT7 elevation, while neither the alcohol dehydrogenase inhibitor (ADH inhi) fomepizole nor the aldehyde dehydrogenase inhibitor (ALDH inhi) daidzin showed any effects (Fig. 6A). We further confirmed these findings by using immunofluorescence (IF) and similar results were observed (Fig. 6B). Next, we measured Cyp2E1 expression after ethanol treatment and found significant induction of Cyp2E1 after 48h of ethanol treatment both in primary human hepatocyte and HepG2 cells (Fig. 6C). To further confirm whether Cyp2E1 was required for ethanol induced SIRT7 elevation, we performed IHC staining in liver sections from wild type (WT) or CyP2E1$^{-/-}$ mice fed with control or alcohol diet (Fig. 6D). In WT mice, alcohol feeding resulted in a significant increase of SIRT7 staining which predominantly localized in nuclei. This increase was not seen with control diet. Consistent with our *in vitro* data, decreased E-cadherin levels were also observed in the liver after alcohol feeding compared with control diet (Fig. 6D). In contrast, in Cyp2E1$^{-/-}$ mice, there were no obvious changes of SIRT7 staining after alcohol feeding compared with control diet and the decrease of E-cadherin levels reduced when compared with WT mice after alcohol (Fig. 6D). Since Cyp2E1 has been suggested as a major contributor to ethanol-induced oxidant stress (8), we thus investigated whether reactive oxygen species (ROS) were responsible for ethanol induced SIRT7 elevation by using N-acetly-cysteine (NAC) as an ROS inhibitor and 4-hydroxynonenal (4-HNE) as an inducer of oxidative stress (Fig. 6E and F). NAC treatment significantly decreased while 4-HNE further enhanced ethanol mediated SIRT7 elevation at mRNA levels (Fig. 6E and F). More importantly, we found that 4-HNE treatment itself was sufficient to increase SIRT7 level in HepG2 cells (Fig. 6G).

Knockdown SIRT7 abolished alcohol mediated HCC metastasis in vivo. The above studies demonstrate that alcohol promotes SIRT7 which is critical for HCC metastasis, suggesting that SIRT7 may play a role in alcohol mediated HCC metastasis. To test this, we first compared SIRT7 and E-cadherin expression in clinical samples (Table. 1) from HCC patients with and without a history of alcohol consumption (Fig. 7A and B). Consistent with our previous observations, SIRT7 expression in alcohol patients was significantly higher than in non-alcohol patients (Fig. 7A, Table 1). IHC staining results indicated mild SIRT7 staining in non-alcohol patients but in alcohol patients, SIRT7 showed strong nuclear and cytosolic staining may due

to post translational modifications caused by alcohol (30) (Fig. 7B). In contrast, E-cadherin expression was significantly decreased in alcohol-associated tumors compared with those from non-alcohol patients (Fig. 7A and B). These results suggest that alcohol consumption modulates SIRT7 and E-cadherin expression in human HCC. To further confirm the role of SIRT7 in alcohol mediated HCC metastasis, we used an established pulmonary metastasis model and fed mice with control diet or alcohol. Due to the high mortality of control mice after 5 weeks alcohol feeding, we fed our mice with alcohol for shorter period of time (2 weeks) one week after tail vein injection (Fig. 7C-E). We found that 2 weeks of alcohol feeding markedly increased lung metastasis compared with those of control diet, evidenced by surface tumor formation (Fig. 7C), IHC staining (Fig. 7D) and tumor number (Fig. 7E). This effect was completely abolished by knockdown of SIRT7 in SK-Hep1 cells with lentiviruses (shSIRT7#2, $p<0.01$). These data clearly indicate that SIRT7 plays a crucial role in alcohol mediated HCC metastasis *in vivo*.

Discussion

Alcohol has long been recognized as a risk factor for liver cancer and long-term alcohol use has been linked to an increased risk of both primary liver tumorigenesis as well as distant metastasis (3–6). Multiple mechanisms seem to be related to alcohol-induced liver cancer tumorigenesis including production of toxic reactive metabolites, oxidative stress and fat accumulation in hepatocyte. These factors all trigger hepatocyte death and promote inflammation(3, 31). Evidence suggests that alcohol use is associated with cancer stem cell activation and EMT, and these facilitate cancer metastasis (6, 9). Nonetheless, additional factors and mechanisms that are responsible for alcohol-mediated liver cancer metastasis remain elusive. In the present study, we have demonstrated that SIRT7 is a pivotal factor which is responsible for alcohol-mediated HCC metastasis. Alcohol upregulates SIRT7 in human HCC and this promotes EMT and increases the risk of metastasis. Knockdown SIRT7 completely abolished alcohol-mediated HCC metastasis *in vivo*. Our data thus provides evidence that SIRT7 induction by CYP2E1-dependent oxidative stress is a molecular mechanism responsible for alcohol-mediated HCC metastasis.

SIRT7 is the most recently identified mammalian sirtuin and growing evidence suggests that its activity is important for human cancer (21, 32–34). High SIRT7 expression is associated with an aggressive cancer phenotype, distant metastasis and poor patient survival in diverse cancers (20, 23, 35, 36). In particular, SIRT7 is important for regulating cancer cell EMT and promoting metastasis, and SIRT7 inactivation reverses metastatic phenotypes in both epithelial and mesenchymal tumors (22, 37, 38). Consistent with these findings, we observed that SIRT7 expression is associated with disease grade in human HCC and high SIRT7 expression showed significant correlation with poor overall and a reduced disease free survival rate. We also demonstrated that SIRT7 is a crucial EMT regulator in HCC and that it promotes cancer cell metastasis. Together with previous work, our findings further highlight the importance of SIRT7 in regulating EMT and maintaining the metastatic phenotype in human HCC.

EMT is the most common feature of advanced cancers, and it initiates metastatic spread (10, 11). In the case of liver cancer, downregulation of E-cadherin expression is the critical molecular feature responsible

for cancer cell EMT(39). While promoter hypermethylation and activation of transcriptional repressors are reported to suppresses E-cadherin (13, 14), our data further revealed that SIRT7 selectively deacetylates H3K18 at the E-cadherin promoter and acts as an E-cadherin repressor in human HCC. We demonstrated that this repression requires FOXO3, a well characterized transcription factor responsible for antioxidant responses and longevity (40). In the absence of FOXO3, SIRT7 no longer suppress E-cadherin transcription. As E-cadherin is a well-documented biomarker of liver cancer prognosis (39, 41), our data suggested that SIRT7 may cooperate with FOXO3 in determining liver cancer progression. Consistent with this, we observed that patients with both high SIRT7 and FOXO3 expression showed the worst survival rate when compared with other expression patterns.

SIRT7 is frequently upregulated in various type of human cancer (42). Studies have been mainly focused on the functional roles and therapeutic options by targeting SIRT7 (23, 35, 36, 43) while mechanisms underlying its regulation have been less well studied. Here we provide evidence that alcohol has the ability to upregulate SIRT7 in both normal liver and human HCC. We further revealed that this upregulation requires CYP2E1 which constitutes the major component of the ethanol oxidizing system. The catalytic activity of the CYP2E1 enzyme results in the generation of ROS which are involved in the initiation and perpetuation of alcohol-associated liver disease. ROS also play a role in signal transduction and cellular physiology to prevent cellular damage (44). Our data indicated that oxidative stress signaling is crucial in alcohol induced SIRT7 upregulation as an anti-oxidant (NAC) prevented and an ROS-induced reactive aldehyde (4-HNE) upregulated SIRT7 mRNA level. Our findings thus provide evidence that ROS serves as a critical factor responsible for alcohol induced SIRT7 upregulation in human HCC. However, even though ROS is a main product of CYP2E1 mediated ethanol oxidation, how ROS activate SIRT7 transcription and whether ROS is primarily responsible for alcohol induced SIRT7 upregulation requires further investigation.

In summary, our data illustrate molecular mechanisms responsible for alcohol-mediated HCC metastasis and demonstrate a crucial role of SIRT7 in alcohol-mediated HCC. Our findings thus highlight the importance of SIRT7 in HCC progression and provide a useful target for the development of mechanism-based cancer therapeutic strategies.

Conclusions

SIRT7-dependent EMT regulation is a pivotal regulatory mechanism of alcohol-mediated HCC metastasis. Therapeutic strategies that inhibit SIRT7 may offer novel options for the treatment of HCC.

Abbreviations

HCC: hepatocellular carcinoma; EMT: epithelial mesenchymal transition; HDAC III: class III histone deacetylation; Sir2: silent information regulator; ChIP: chromatin immunoprecipitation; IHC: immunohistochemistry; TCGA: The Cancer Genome Altas; ALD: acetaldehyde; ALDH: aldehyde

dehydrogenase ; ADH: alcohol dehydrogenase; IF: immunofluorescence; ROS: reactive oxygen species; NAC: N-acetly-cysteine; 4-HNE: 4-hydroxynonenal.

Declarations

ETHICS APPROVAL AND CONSENT TO PARTICIPATE

All animal handing procedures were approved by the Institutional Animal Care and Use

Committees at The University of Kansas Medical Center and Hunan Normal University. Liver specimens were obtained from the University of Kansas Medical Center, the First Affiliated Hospital of Chongqing Medical University, and the Affiliated Hospital of Hunan Normal University. Written informed consent was obtained from all patients and all studies using human tissue samples were approved by the Human Subjects Committee of the University of Kansas Medical Center, Chongqing Medical University and Hunan Normal University School of Medicine.

CONSENT FOR PUBLICATION

Not applicable.

AVAILABILITY OF DATA AND MATERIALS

All data generated or analyzed during this study are included in this published article.

COMPETING INTERESTS

The authors declare that they have no financial conflicts of interest relevant to this study.

FUNDING

This study was supported by grant 81974458, 82170607 from the National Natural Science Foundation of China, grant 2021JJ30463 from Hunan Provincial Natural Science Foundation of China, grant 2019RS1042, 2018RS3072 from the China Hunan Provincial Science/Technology Department, grant P30 GM118247 from the National Institute of General Medical Sciences from the National Institutes of Health (USA) and a startup grant from Hunan Normal University. Grants AA026025 and AA012863 to SAW from the National Institute on Alcohol Abuse and Alcoholism of the National Institutes of Health (USA).Jinqiu Zhao was supported by grant CSTC2020JCYJ-MSXMX0224 from Chongqing Natural Science Foundation. The specimens used in this study were provided, in part, by the University of Kansas Liver Center Biorepository.

AUTHORS' CONTRIBUTIONS

ZL, CZ, JQZ and JZ performed experiments and acquired data. BHL, WBT and YL collected clinical samples, performed immunoassays and statistical analysis. ZL, WXH and SW conceived of the study,

and participated in its design and coordination. ZL and SW analyzed data and wrote the paper. All authors had edited and approved the final manuscript.

ACKNOWLEDGE

The authors acknowledge Dr Laura Nagy (Cleveland Clinic) who provide key material for this study, contribution of the patients who donated specimens for research as well as the physicians, nurses and researchers who procured the specimens.

References

1. Altekruse SF, McGlynn KA, Reichman ME. Hepatocellular carcinoma incidence, mortality, and survival trends in the United States from 1975 to 2005. J Clin Oncol. 2009;27(9):1485-91.
2. Aravalli RN, Steer CJ, Cressman EN. Molecular mechanisms of hepatocellular carcinoma. Hepatology. 2008;48(6):2047-63.
3. Parker R, Kim SJ, Gao B. Alcohol, adipose tissue and liver disease: mechanistic links and clinical considerations. Nature reviews Gastroenterology & hepatology. 2018;15(1):50-9.
4. Huang CS, Ho CT, Tu SH, Pan MH, Chuang CH, Chang HW, et al. Long-term ethanol exposure-induced hepatocellular carcinoma cell migration and invasion through lysyl oxidase activation are attenuated by combined treatment with pterostilbene and curcumin analogues. Journal of agricultural and food chemistry. 2013;61(18):4326-35.
5. Brandon-Warner E, Walling TL, Schrum LW, McKillop IH. Chronic Ethanol Feeding Accelerates Hepatocellular Carcinoma Progression in a Sex-Dependent Manner in a Mouse Model of Hepatocarcinogenesis. Alcoholism-Clinical and Experimental Research. 2012;36(4):641-53.
6. Szabo G. Alcoholic Liver Disease Accelerates Early Hepatocellular Cancer in a Mouse Model. Advances in experimental medicine and biology. 2018;1032:71-9.
7. McKillop IH, Schrum LW. Role of alcohol in liver carcinogenesis. Seminars in liver disease. 2009;29(2):222-32.
8. Lu Y, Cederbaum AI. CYP2E1 and oxidative liver injury by alcohol. Free Radic Biol Med. 2008;44(5):723-38.
9. Chen DL, Yu DD, Wang XY, Liu Y, He YJ, Deng RQ, et al. Epithelial to mesenchymal transition is involved in ethanol promoted hepatocellular carcinoma cells metastasis and stemness. Mol Carcinog. 2018;57(10):1358-70.
10. Acloque H, Adams MS, Fishwick K, Bronner-Fraser M, Nieto MA. Epithelial-mesenchymal transitions: the importance of changing cell state in development and disease. The Journal of clinical investigation. 2009;119(6):1438-49.
11. Thiery JP, Acloque H, Huang RY, Nieto MA. Epithelial-mesenchymal transitions in development and disease. Cell. 2009;139(5):871-90.

12. van Zijl F, Zulehner G, Petz M, Schneller D, Kornauth C, Hau M, et al. Epithelial-mesenchymal transition in hepatocellular carcinoma. Future Oncol. 2009;5(8):1169-79.
13. Larue L, Bellacosa A. Epithelial-mesenchymal transition in development and cancer: role of phosphatidylinositol 3' kinase/AKT pathways. Oncogene. 2005;24(50):7443-54.
14. Yoshida J, Horiuchi A, Kikuchi N, Hayashi A, Osada R, Ohira S, et al. Changes in the expression of E-cadherin repressors, Snail, Slug, SIP1, and Twist, in the development and progression of ovarian carcinoma: the important role of Snail in ovarian tumorigenesis and progression. Med Mol Morphol. 2009;42(2):82-91.
15. Ford E, Voit R, Liszt G, Magin C, Grummt I, Guarente L. Mammalian Sir2 homolog SIRT7 is an activator of RNA polymerase I transcription. Genes Dev. 2006;20(9):1075-80.
16. Vakhrusheva O, Smolka C, Gajawada P, Kostin S, Boettger T, Kubin T, et al. Sirt7 increases stress resistance of cardiomyocytes and prevents apoptosis and inflammatory cardiomyopathy in mice. Circ Res. 2008;102(6):703-10.
17. Ryu D, Jo YS, Lo Sasso G, Stein S, Zhang H, Perino A, et al. A SIRT7-dependent acetylation switch of GABPbeta1 controls mitochondrial function. Cell metabolism. 2014;20(5):856-69.
18. Li Z, Bridges B, Olson J, Weinman SA. The interaction between acetylation and serine-574 phosphorylation regulates the apoptotic function of FOXO3. Oncogene. 2017;36(13):1887-98.
19. Chen S, Blank MF, Iyer A, Huang B, Wang L, Grummt I, et al. SIRT7-dependent deacetylation of the U3-55k protein controls pre-rRNA processing. Nature communications. 2016;7:10734.
20. Barber MF, Michishita-Kioi E, Xi Y, Tasselli L, Kioi M, Moqtaderi Z, et al. SIRT7 links H3K18 deacetylation to maintenance of oncogenic transformation. Nature. 2012;487(7405):114-8.
21. Kim JK, Noh JH, Jung KH, Eun JW, Bae HJ, Kim MG, et al. Sirtuin7 oncogenic potential in human hepatocellular carcinoma and its regulation by the tumor suppressors MiR-125a-5p and MiR-125b. Hepatology (Baltimore, Md). 2013;57(3):1055-67.
22. Malik S, Villanova L, Tanaka S, Aonuma M, Roy N, Berber E, et al. SIRT7 inactivation reverses metastatic phenotypes in epithelial and mesenchymal tumors. Scientific reports. 2015;5:9841.
23. Zhao J, Wozniak A, Adams A, Cox J, Vittal A, Voss J, et al. SIRT7 regulates hepatocellular carcinoma response to therapy by altering the p53-dependent cell death pathway. Journal of experimental & clinical cancer research : CR. 2019;38(1):252.
24. Li Z, Zhao J, Tikhanovich I, Kuravi S, Helzberg J, Dorko K, et al. Serine 574 phosphorylation alters transcriptional programming of FOXO3 by selectively enhancing apoptotic gene expression. Cell Death Differ. 2016;23(4):583-95.
25. Li Z, Zhao J, Zhang S, Weinman SA. FOXO3-dependent apoptosis limits alcohol-induced liver inflammation by promoting infiltrating macrophage differentiation. Cell Death Discov. 2018;4:16.
26. Sebastian BM, Roychowdhury S, Tang H, Hillian AD, Feldstein AE, Stahl GL, et al. Identification of a cytochrome P4502E1/Bid/C1q-dependent axis mediating inflammation in adipose tissue after chronic ethanol feeding to mice. The Journal of biological chemistry. 2011;286(41):35989-97.

27. Xie Y, McGill MR, Dorko K, Kumer SC, Schmitt TM, Forster J, et al. Mechanisms of acetaminophen-induced cell death in primary human hepatocytes. Toxicology and applied pharmacology. 2014;279(3):266-74.
28. McKillop IH, Schrum LW, Thompson KJ. Role of alcohol in the development and progression of hepatocellular carcinoma. Hepatic oncology. 2016;3(1):29-43.
29. Yin H, Hu M, Liang X, Ajmo JM, Li X, Bataller R, et al. Deletion of SIRT1 from hepatocytes in mice disrupts lipin-1 signaling and aggravates alcoholic fatty liver. Gastroenterology. 2014;146(3):801-11.
30. Parira T, Figueroa G, Laverde A, Casteleiro G, Gomez Hernandez ME, Fernandez-Lima F, et al. Novel detection of post-translational modifications in human monocyte-derived dendritic cells after chronic alcohol exposure: Role of inflammation regulator H4K12ac. Scientific reports. 2017;7(1):11236.
31. Tan HK, Yates E, Lilly K, Dhanda AD. Oxidative stress in alcohol-related liver disease. World journal of hepatology. 2020;12(7):332-49.
32. Wang HL, Lu RQ, Xie SH, Zheng H, Wen XM, Gao X, et al. SIRT7 Exhibits Oncogenic Potential in Human Ovarian Cancer Cells. Asian Pac J Cancer Prev. 2015;16(8):3573-7.
33. Zhang S, Chen P, Huang Z, Hu X, Chen M, Hu S, et al. Sirt7 promotes gastric cancer growth and inhibits apoptosis by epigenetically inhibiting miR-34a. Sci Rep. 2015;5:9787.
34. Paredes S, Villanova L, Chua KF. Molecular pathways: emerging roles of mammalian Sirtuin SIRT7 in cancer. Clin Cancer Res. 2014;20(7):1741-6.
35. Yu HY, Ye W, Wu JX, Meng XQ, Liu RY, Ying XF, et al. Overexpression of Sirt7 Exhibits Oncogenic Property and Serves as a Prognostic Factor in Colorectal Cancer. Clinical Cancer Research. 2014;20(13):3434-45.
36. Li H, Tian Z, Qu Y, Yang Q, Guan H, Shi B, et al. SIRT7 promotes thyroid tumorigenesis through phosphorylation and activation of Akt and p70S6K1 via DBC1/SIRT1 axis. Oncogene. 2019;38(3):345-59.
37. Monteiro-Reis S, Lameirinhas A, Miranda-Goncalves V, Felizardo D, Dias PC, Oliveira J, et al. Sirtuins' Deregulation in Bladder Cancer: SIRT7 Is Implicated in Tumor Progression through Epithelial to Mesenchymal Transition Promotion. Cancers. 2020;12(5).
38. Zhao Y, Ye X, Chen R, Gao Q, Zhao D, Ling C, et al. Sirtuin 7 promotes nonsmall cell lung cancer progression by facilitating G1/S phase and epithelialmesenchymal transition and activating AKT and ERK1/2 signaling. Oncol Rep. 2020;44(3):959-72.
39. Loh CY, Chai JY, Tang TF, Wong WF, Sethi G, Shanmugam MK, et al. The E-Cadherin and N-Cadherin Switch in Epithelial-to-Mesenchymal Transition: Signaling, Therapeutic Implications, and Challenges. Cells-Basel. 2019;8(10).
40. Brunet A, Sweeney LB, Sturgill JF, Chua KF, Greer PL, Lin Y, et al. Stress-dependent regulation of FOXO transcription factors by the SIRT1 deacetylase. Science (New York, NY). 2004;303(5666):2011-5.
41. Han LL, Jia L, Wu F, Huang C. Sirtuin6 (SIRT6) Promotes the EMT of Hepatocellular Carcinoma by Stimulating Autophagic Degradation of E-Cadherin. Molecular cancer research : MCR. 2019;17(11):2267-80.

42. Blank MF, Grummt I. The seven faces of SIRT7. Transcription. 2017;8(2):67-74.
43. Tang X, Shi L, Xie N, Liu Z, Qian M, Meng F, et al. SIRT7 antagonizes TGF-beta signaling and inhibits breast cancer metastasis. Nature communications. 2017;8(1):318.
44. Leung TM, Nieto N. CYP2E1 and oxidant stress in alcoholic and non-alcoholic fatty liver disease. Journal of hepatology. 2013;58(2):395-8.

Tables

Table 1 Correlative analysis of alcohol consumption with SIRT7 levels or clinicopathological features by using a nonparametric Fisher's Exact Test.

Clinicopatholigic Parameters	Number of specimens	Alcohol		P value
		Yes	No	
Sex				0.7806
Female	8	0	8	
Male	11	8	3	
Age(mean±SD)		61±9.62	50.1±19.59	0.1534
Tumor size				0.6491
>3cm	16	10	6	
<3cm	3	2	1	
Multiple Tumor				0.3251
YES	4	1	3	
NO	15	2	13	
Vascular invasion				0.2482
YES	5	1	4	
NO	14	2	12	
Stage				0.3308
I	2	1	1	
II	7	4	3	
III	7	2	5	
IV	3	0	3	
SIRT7 expression				0.0186
High	9	7	2	
Low	8	2	6	

Figures

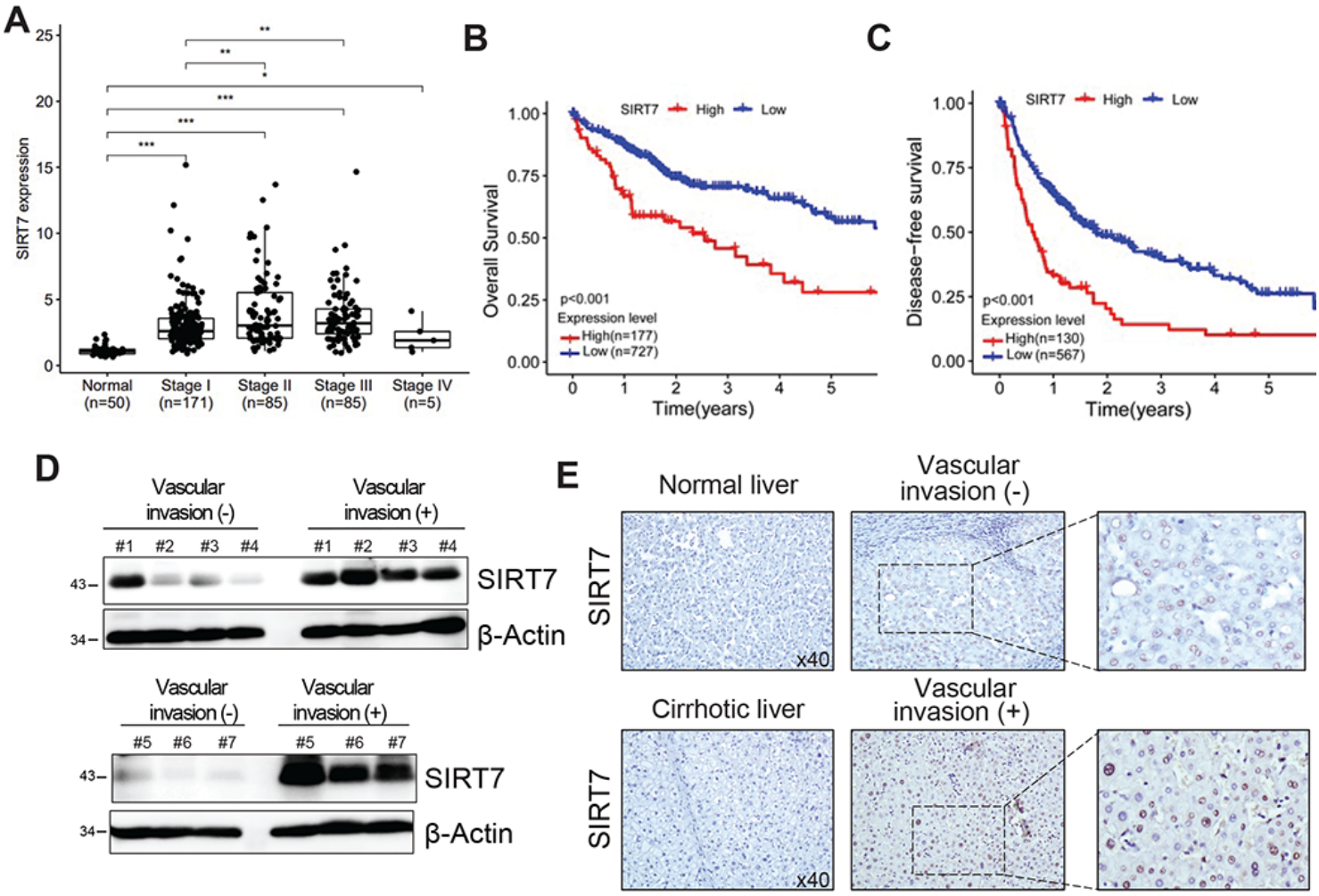

Figure 1

Elevated SIRT7 expression in human HCC and associated with poor prognosis. (A) Analysis of SIRT7 mRNA expression in normal tissue (n=50) and differential stage based on TNM classification of HCC (n = 336) using the data from the TCGA public database. (B-C) Kaplan–Meier analysis of overall survival (n= 904) and disease free survival (n=697) in liver cancer patients based on SIRT7 expression and used mean as cut-off value for high and low expression. (D) Western blot analysis of SIRT7 protein levels in primary and metastatic HCC. Numbers indicate individual patients. (E) Representative IHC staining for protein levels of SIRT7 in normal, cirrhotic, primary and metastatic HCC liver sections.

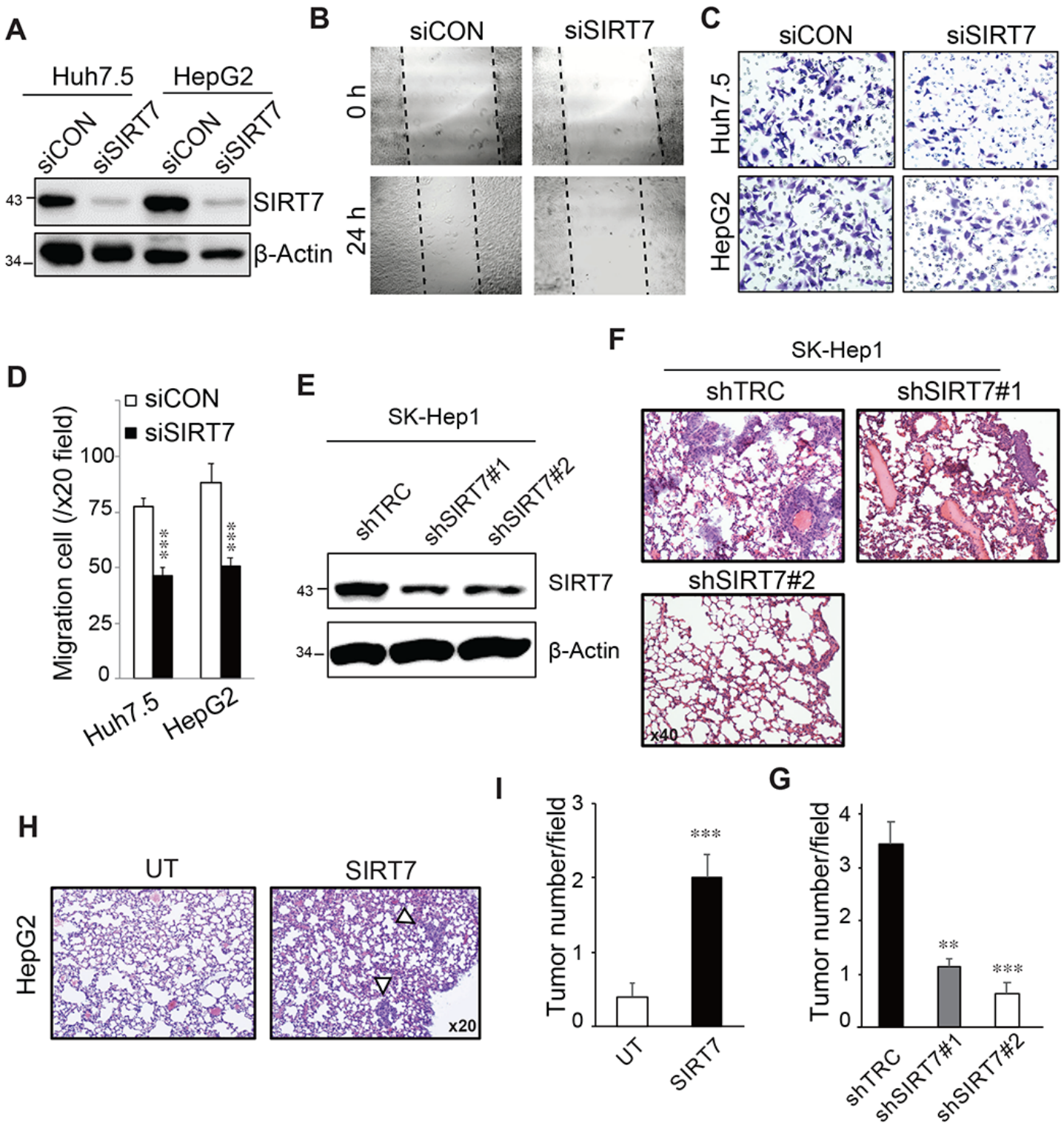

Figure 2

SIRT7 promotes HCC metastasis. (A) Huh7.5 and HepG2 cells were treated with siRNA targeting SIRT7 (siSIRT7) for 72 h, protein levels of SIRT7 were evaluated by WB, cell migration were evaluated by using wound healing (B) and migration assay (C, D). (E) Knockdown efficiency of SK-Hep1 cells were treated with scramble (shTRC) or shRNA targeting SIRT7 (shSIRT7) for 72 hours. (F) 1x106 cells in E were injected into NSG mice via tail vein injection, tumor formation was determined in lung 4 weeks after

injection by using H&E staining and quantified data shown in G. (H-I) HepG2 cells were transfected with SIRT7 for 24 h and then 1x106 cells were injected into NSG mice via tail vein injection, tumor formation was determined in lung 4 weeks after injection by using H&E staining in lung tissues and quantified data shown in I. Graphs show mean ± SEM of at least three independent experiments. **P<0.01, ***P<0.001, Student's t-test.

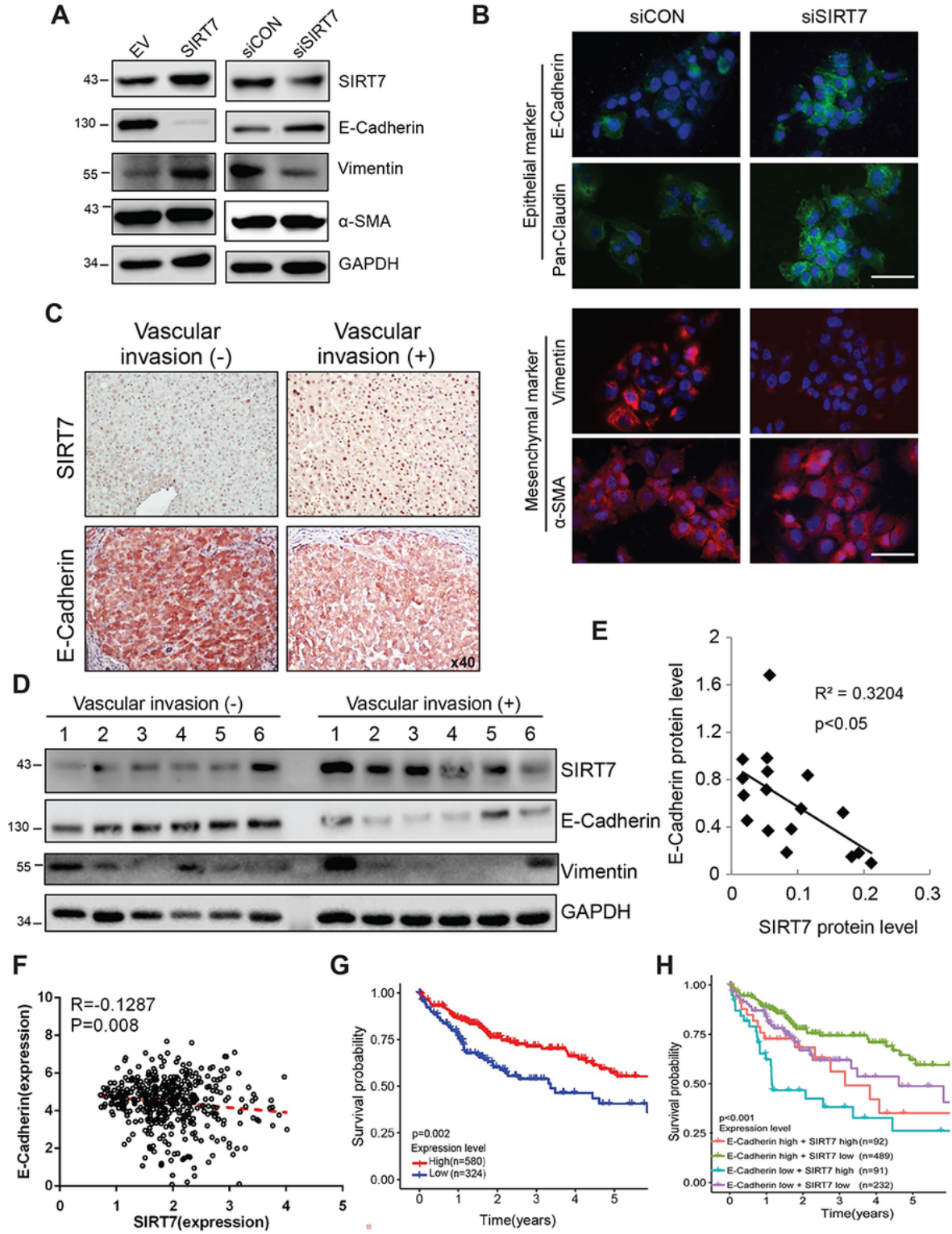

Figure 3

SIRT7 regulates EMT of HCC cells. (A) Huh7.5 cells were transfected with SIRT7 or siSIRT7. Protein levels of EMT related genes were evaluated by western blot by using antibodies as indicated. (B) Immunofluorescence for epithelial cell marker (Green) and mesenchymal cell marker (red) in cells treated with siSIRT7 as in A. Scale bar indicates 50 μm. (C-D) Representative IHC staining (C) and WB analysis (D) for SIRT7 and E-cadherin primary and metastatic HCC liver sections. (E) Spearman correlation between SIRT7 and E-cadherin expression as in D ($R=-0.566$, $p<0.05$). (F) Spearman correlation between SIRT7 and E-cadherin mRNA expression using the data from the TCGA public database. ($R=-0.129$, $p<0.01$). (G-H) Kaplan–Meier analysis of overall survival in liver cancer patients based on E-cadherin (G) or SIRT7 and E-cadherin (H) expression by using mean as cut-off values.

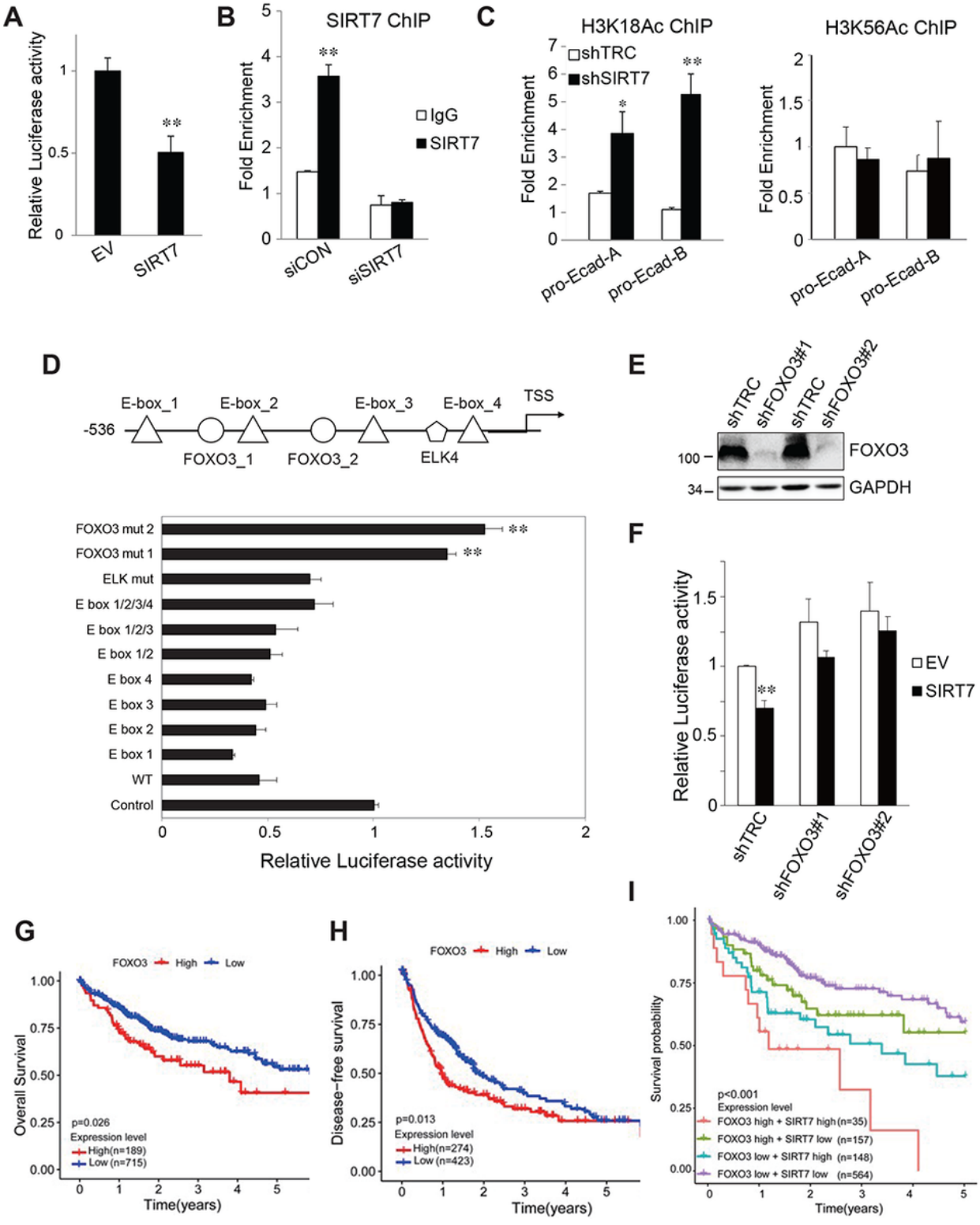

Figure 4

SIRT7 induces H3K18 deacetylation and suppresses E-cadherin via FOXO3. (A) Luciferase activity from Huh7.5 were transfected with luciferase reporter plasmid containing E-cadherin promoter with empty vector (EV) or Flag-SIRT7. **P<0.01, Student's t-test. (B) Huh7.5 cells were transfected with nontargeted siRNA (siCON) or siRNA targeting SIRT7 (siSIRT7). ChIP assay was performed with SIRT7 antibody. **P<0.01 vs IgG, Student's t-test. (C) Huh7.5 cells were treated with scramble (shTRC) or shRNA targeting

SIRT7 (shSIRT7) for 72 hours, acetylation levels within promoter regions of E-cadherin (pro-Ecah-A and pro-Ecah-B) were measured by ChIP assay by using antibodies as indicated. **P<0.01 vs IgG, Student's t-test. (D) Luciferase assays from Huh7.5 were transfected with Flag-SIRT7 and luciferase reporter plasmid containing E-cadherin promoter (WT) or promoters with mutations of E-box, ELK4 or FOXO3 binding sites as indicated. **P<0.01 vs WT, One way ANOVA. (E) Huh7.5 cells were treated with scramble (shTRC) or shRNA targeting FOXO3 (shFOXO3) for 72 hours, Protein level of FOXO3 were evaluated by WB. (D) Luciferase assays from cells in E were transfected with luciferase reporter plasmid containing E-cadherin promoter and empty vector (EV) or Flag-SIRT7. **P<0.01 vs EV, Student's t-test. All graphs show mean ± SEM of at least three independent experiments.

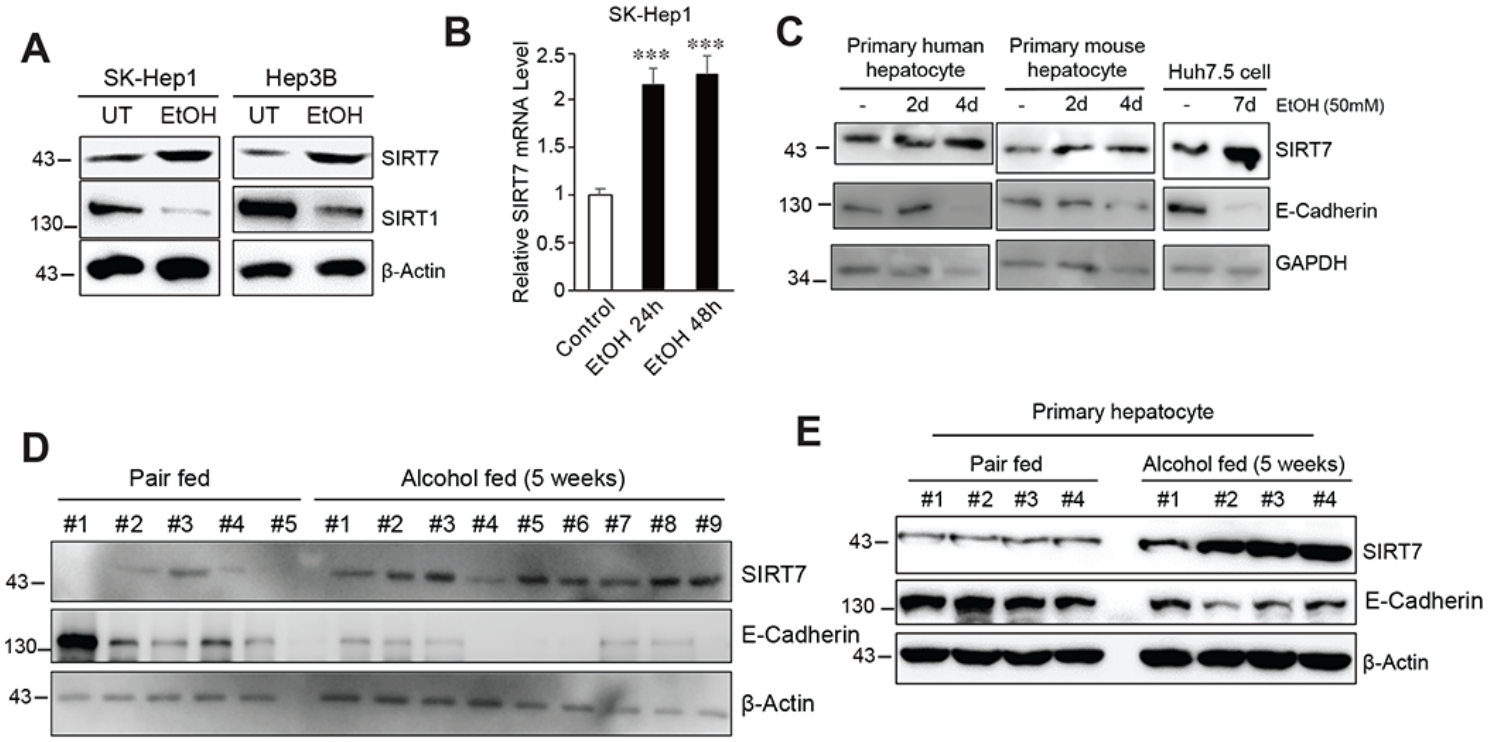

Figure 5

EtOH upregulates SIRT7 expression. (A) Western blot analysis of SIRT7 protein levels SK-Hep1 and Hep3B cell after EtOH treatment (50mM) for 48h. (B) mRNA levels of SIRT7 after EtOH (50 mM) treatment at various of time as indicated. Graphs show mean ± SEM of at least three independent experiments, ***P<0.001, One way ANOVA. (C) Protein levels of SIRT7 and E-cadherin after EtOH (50 mM) treatment in primary hepatocytes and Huh7.5 cells at various of time as indicated. (D) Protein levels of SIRT7 and E-cadherin in liver (D) or primary mouse hepatocyte (E) from mice were pair-fed or fed with alcohol for 5 weeks.

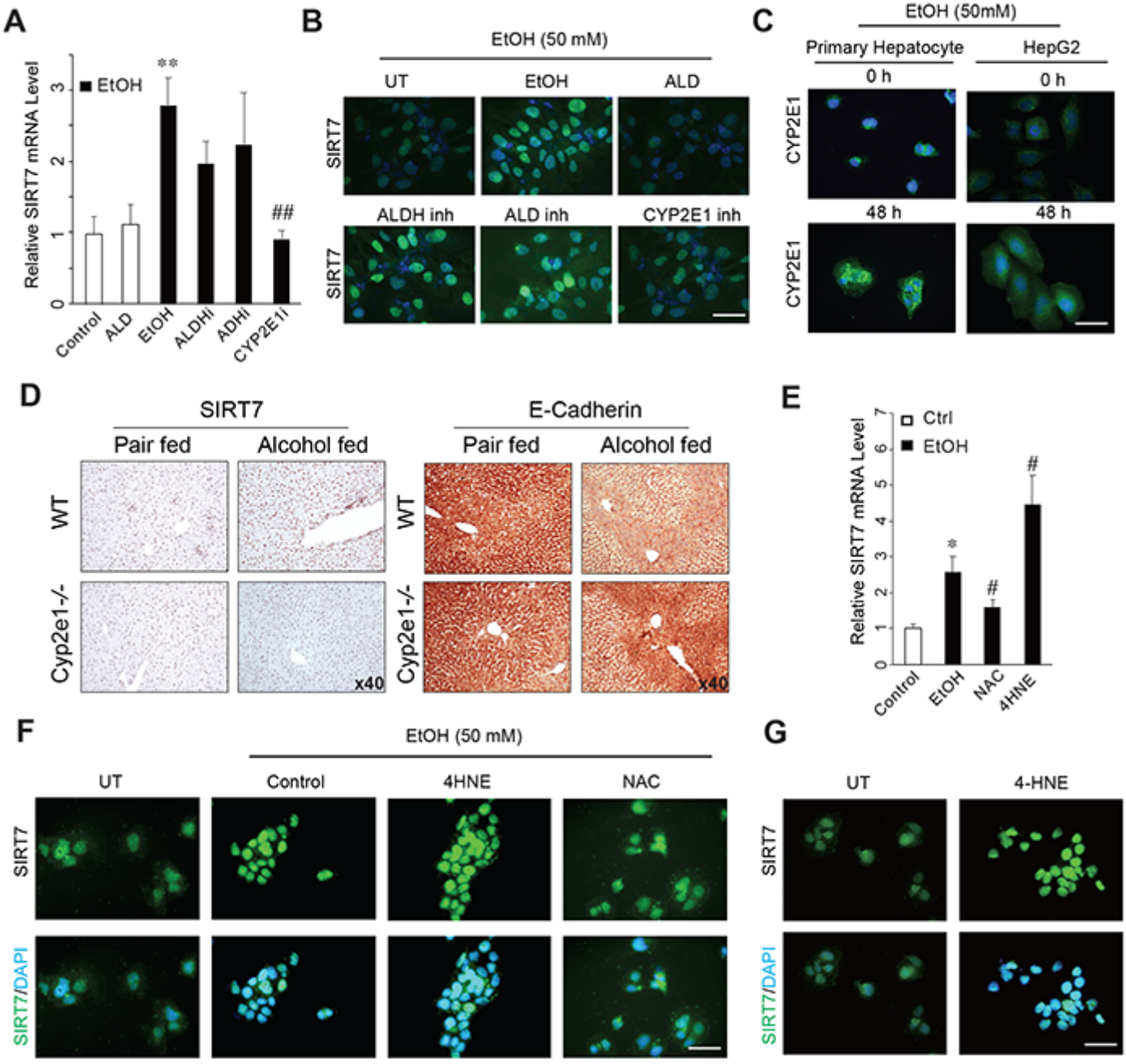

Figure 6

Cyp2E1-dependent oxidative stress is responsible for alcohol mediated SIRT7 induction. (A) Hep3B were untreated (Control), treated with aldehyde (ALD), or EtOH in the absence or present of fomepizole (ADH inhi), daidzin (ALDH inhi), or alizarin (Cyp2E1 inhi) for 24h and SIRT7 mRNA level were evaluated by qRT-PCR. Graphs show mean ± SEM of at least three independent experiments, **P<0.001 vs Control, ##P<0.001 vs EtOH, One way ANOVA. (B) Immunofluorescence for SIRT7 protein (Green) in cells as in A. Scale bar indicates 50 μm. (C) Immunofluorescence for Cyp2E1 protein (Green) in primary hepatocytes and HepG2 cells treated with EtOH for 48h. Scale bar indicates 50 μm. (D) Representative IHC staining of SIRT7 and E-cadherin in WT and Cyp2E1-/- mice were pair- or alcohol-fed for 5 weeks. (E) Hep3B were untreated (Control) or treated with EtOH in the absence or present of N-acetly-cysteine (NAC) or 4-hydroxynonenal (4-HNE) for 24h, mRNA levels of SIRT7 were evaluated by qRT-PCR. Graphs show mean ±

SEM of at least three independent experiments, *P<0.05 vs Control, #P<0.05 vs EtOH, One way ANOVA. (F) Immunofluorescence for SIRT7 protein (Green) in cells as in E. Scale bar indicates 50 μm. (G) Immunofluorescence for SIRT7 protein (Green) in Hep3B cells were treated with 4-HNE for 24h. Scale bar indicates 50 μm.

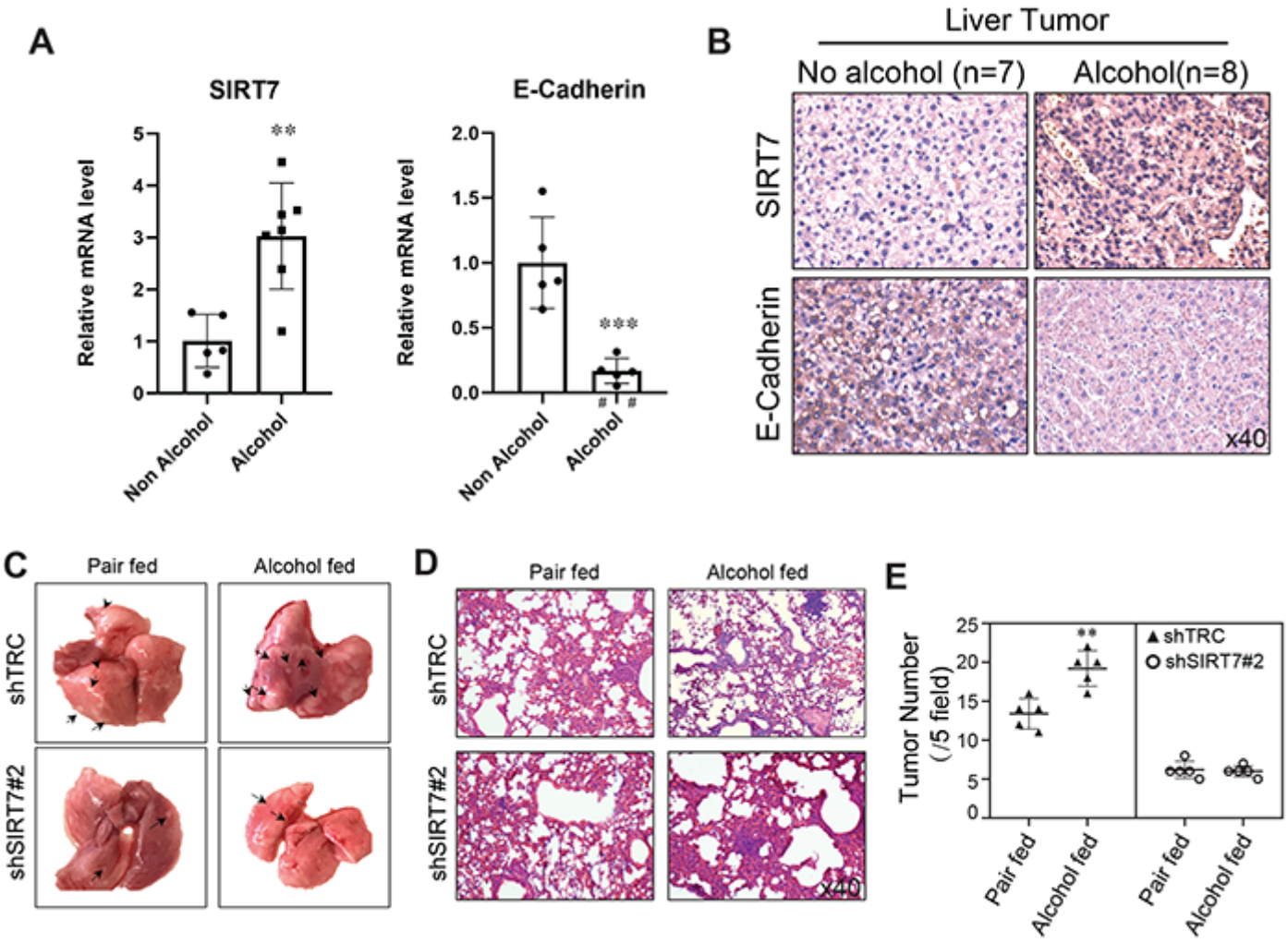

Figure 7

Knockdown SIRT7 prevents alcohol mediated HCC metastasis. (A) Analysis of SIRT7 and E-cadherin mRNA levels in HCC with (n=7) or without (n=5) alcohol consumption. Data are presented as the mean ± SEM, **P<0.01, ***P<0.001, Student's t-test. (B) Representative IHC staining for protein levels of SIRT7 and E-cadherin in liver sections from HCC patients with (n=8) or without (n=9) alcohol consumption. (C-E) SK-Hep1 cells were treated with scramble (shTRC) or shRNA targeting SIRT7 (shSIRT7) for 72 hours, 1x106 cells were injected into NSG mice via tail vein injection and one week after injection, mice were pair or alcohol for 2 more weeks, gross image (C) and H&E stained (D) lung tissues that showed metastasized HCC cell mass and quantified data shown in E. Data are presented as the mean ± SEM,**P<0.01 vs pair fed/shTRC, one way ANOVA.